LETTERS

Gating charge displacement in voltage-gated ion channels involves limited transmembrane movement

Baron Chanda[1], Osei Kwame Asamoah[1]†, Rikard Blunck[1], Benoît Roux[2] & Francisco Bezanilla[1,3]

Voltage-gated ion channels are responsible for generating electrical impulses in nerves and other excitable cells. The fourth transmembrane helix (S4) in voltage-gated channels is the primary voltage-sensing unit that mediates the response to a changing membrane electric field[1,2]. The molecular mechanism of voltage sensing, particularly with respect to the magnitude of the transmembrane movement of S4, remains controversial[3–5]. To determine the extent of this transmembrane movement, we use fluorescent resonance energy transfer between the S4 domain and a reference point in the lipid bilayer. The lipophilic ion dipicrylamine distributes on either side of the lipid bilayer depending on the membrane potential, and is used here as a resonance-energy-transfer acceptor from donor molecules attached to several positions in the Shaker K^+ channel. A voltage-driven transmembrane movement of the donor should produce a transient fluorescence change because the acceptor also translocates as a function of voltage. In Shaker K^+ channels no such transient fluorescence is observed, indicating that the S4 segment does not translocate across the lipid bilayer. Based on these observations, we propose a molecular model of voltage gating that can account for the observed 13*e* gating charge with limited transmembrane S4 movement.

Molecular models of voltage gating that invoke a large translocation of the voltage-sensing S4 segment, such as the 'helical screw'[6,7] (in its original form) or the 'paddle'[5,8] models, account for the observed 13*e* gating charges intuitively by incorporating a complete translocation of the charged S4 residues across the full thickness of the lipid membrane. For example, in the paddle model the gating charges of the S4 segment are buried in the lipid bilayer and traverse approximately 20 Å in response to a transmembrane potential change. However, accessibility data[9–12], resonance energy transfer[13,14] and potentiometric studies[15] suggest that the voltage sensor undergoes relatively small transmembrane excursions. Previous measurements of the extent of the voltage sensor's translocation using fluorescent resonance energy transfer (FRET) did not resolve this issue because the distance estimates were obtained by measuring relative distances between mobile voltage sensors[13,14]. Our aim is to determine whether, during the gating process, the main voltage-sensing element (S4) undergoes a small or a large transmembrane movement relative to the membrane plane. To address this issue, we use the lipid bilayer as an independent reference plane and a novel strategy based on FRET.

The non-fluorescent hydrophobic anion dipicrylamine (DPA) (Fig. 1a, inset), which localizes at the lipid-aqueous interface, can be used as a classical Förster-energy-transfer acceptor from a variety of donor fluorophores owing to its absorbance in the blue region of the visible spectrum. In response to a change in membrane potential, DPA generates robust gating currents as it moves between the inner and outer membrane leaflets (Fig. 1b). The voltage- and time-dependent FRET signal ($\Delta F/F$) that arises from donor fluorescence quenching in the presence of DPA reflects the magnitude and direction of movement that is normal to the bilayer plane. If the S4 segment remains relatively static during the gating process (Fig. 1c, left), the donor fluorescence at the beginning of the pulse is quenched by the presence of DPA molecules that accumulate in the outer leaflet. Upon depolarization, the fluorescence increases monotonically because only DPA migrates to the inner leaflet of the lipid bilayer. Conversely, if the S4 segment also translocates across the membrane, the FRET signal is more complex (Fig. 1c, right). At hyperpolarized potentials, the S4 segment resides near the inner leaflet while DPA molecules populate the outer leaflet. Upon depolarization, the DPA molecules quickly migrate to the inner leaflet and quench the donor fluorescence. As the S4 segment subsequently moves towards the outer membrane the donor fluorescence recovers. This interplay results in a characteristic biphasic time trace with the donor fluorescence returning to baseline on sustained depolarization. We note that the biphasic time trace is observed even when both donor and acceptor groups have equal charge and mobility in the membrane, as long as they translocate from one side of the bilayer to the other (Supplementary Discussion). Thus, the fluorescence profile (biphasic versus monophasic) generated by such FRET pairs can provide a stringent qualitative test to discriminate between the two contrasting gating models.

We performed a series of control experiments in native *Xenopus laevis* oocyte membranes to validate this FRET technique. To reproduce the model of a large S4 translocation, the lipophilic anionic fluorophore oxonol (bis-(1,3-diethylthiobarbituric acid)trimethine oxonol; also called $DiSBAC_2$) was employed as a FRET donor. Because oxonol translocates across the bilayer with a time constant of 300 ms at 0 mV (ref. 16), 350-fold slower than DPA, we expect a transient FRET signal owing to this large difference in translocation time. Upon depolarization, the oxonol fluorescence shows an initial increase that is consistent with reduced FRET efficiency as DPA migrates away from oxonol. As oxonol molecules slowly relocate to the inner membrane leaflet, a decrease in fluorescence is observed. Upon repolarization, an analogous optical signal is observed as the hydrophobic anions re-establish their original positions (Fig. 1d). In contrast, a monotonic FRET signal is observed upon depolarization from di-8-ANEPPS (see Methods), which is a potentiometric dye that is exclusively localized to the outer leaflet

[1]Departments of Physiology and Anesthesiology, David Geffen School of Medicine, UCLA, 650 Charles E. Young Dr. South, Los Angeles, California 90025, USA. [2]Department of Physiology and Biophysics, Weill Medical College, Cornell University, 1300 York Avenue, New York, New York 10021, USA. [3]Centro de Estudios Cientificos, Valdivia, Chile.
†Present address: Department of Emergency Medicine, University of New Mexico Health Sciences Campus, Albuquerque, New Mexico 87106, USA.

(Fig. 1e, top). A small intrinsic electrochromic signal from di-8-ANEPPS (Fig. 1e, bottom) is overwhelmed by the FRET signal in the presence of DPA. As a further test, we used fluorescently labelled melittin peptide[17] for which there is evidence of voltage-activated insertion or translocation across the membrane upon hyperpolarization; akin to the paddle model[18]. When the potential was stepped to inside negative (see Methods), the fluorescence showed an early decrease corresponding to the translocation of DPA molecules (Fig. 1f). On sustained hyperpolarization, the fluorescence recovers with a time course that correlates with increasing membrane conductance, and reflects the formation of functional melittin channels. Thus, the transient FRET signal supports the hypothesis that the amino terminus of melittin moves across the width of the bilayer in response to a voltage pulse (Supplementary Discussion). Taken together, these results confirm that this FRET approach can distinguish a large transmembrane movement of protein segments from a minimal movement.

The extent of voltage-sensor translocation in Shaker K^+ channels was determined by measuring FRET signals from different positions in the S4 segment relative to DPA in the membrane. Our measurements were limited to residues D349, Q354, V363, V367 and F425, as these sites generate small (if any) intrinsic voltage-dependent fluorescence signals (Supplementary Discussion). The fluorescent label sulphorhodamine was attached using a methanethiosulphonate (MTS) linker to the cysteine-substituted residues in the S4 segment of the cysteine-less Shaker channels. FRET signals were recorded in response to a single voltage pulse to +50 mV (from −120 mV). This protocol is expected to move all gating charge in the Shaker channels, together with the majority of DPA molecules, across the bilayer. FRET signals from D349C and Q354C, close to the N terminus of S4, show a clear monophasic fluorescence increase consistent with their static position (Fig. 2a). FRET signals from V363C (close to the charge-carrying residues) is also monophasic, but inverted in orientation relative to the signals from the previous sites, suggesting that this site lies closer to the inner leaflet. This was initially surprising, because the neighbouring R362 residue is the first charge-carrying residue and is expected to be close to the outer membrane surface. However, the inverted signal is probably due to the long length of the sulphorhodamine dipole midpoint (~10 Å). This results in a shorter DPA–chromophore distance when DPA populates the inner (as compared to outer) membrane (Fig. 2b and Supplementary Discussion). The energy-transfer midline, as defined by FRET orientation, is unlikely to coincide with the physical midline of the lipid bilayer. For instance, if the footprint of the channel protein on the outer leaflet is larger than that on the inner leaflet, the energy-transfer midline is biased towards the outer leaflet. Thus, inverted FRET signals from V363C may reflect the long chromophore length, channel geometry and/or orientation of the voltage sensor. Nonetheless, it clearly does not produce the transient fluorescence signal expected from a group that translocates across the bilayer. The V367C residue, located before the third gating charge in the S4 segment and below V363C, also shows a monophasic decrease in fluorescence. As a control for fixed position, F425C (close to outer pore) was tested; it showed a monophasic fluorescence increase.

To further constrain the movement of S4 during gating, we labelled residue V363C with a 7-fluorobenz-2-oxa-1,3-diazole-4-sulphonamide (ABD) group using an MTS linker. The ABD chromophore is extremely sensitive to its environment and its electrical dipole midpoint is only 6 Å from the thiol group. The FRET signals between ABD–V363C and DPA in the membrane is monophasic, but reversed in direction relative to sulphorhodamine at the same position (Fig. 2c). This indicates that the ABD chromophore, unlike sulpho-

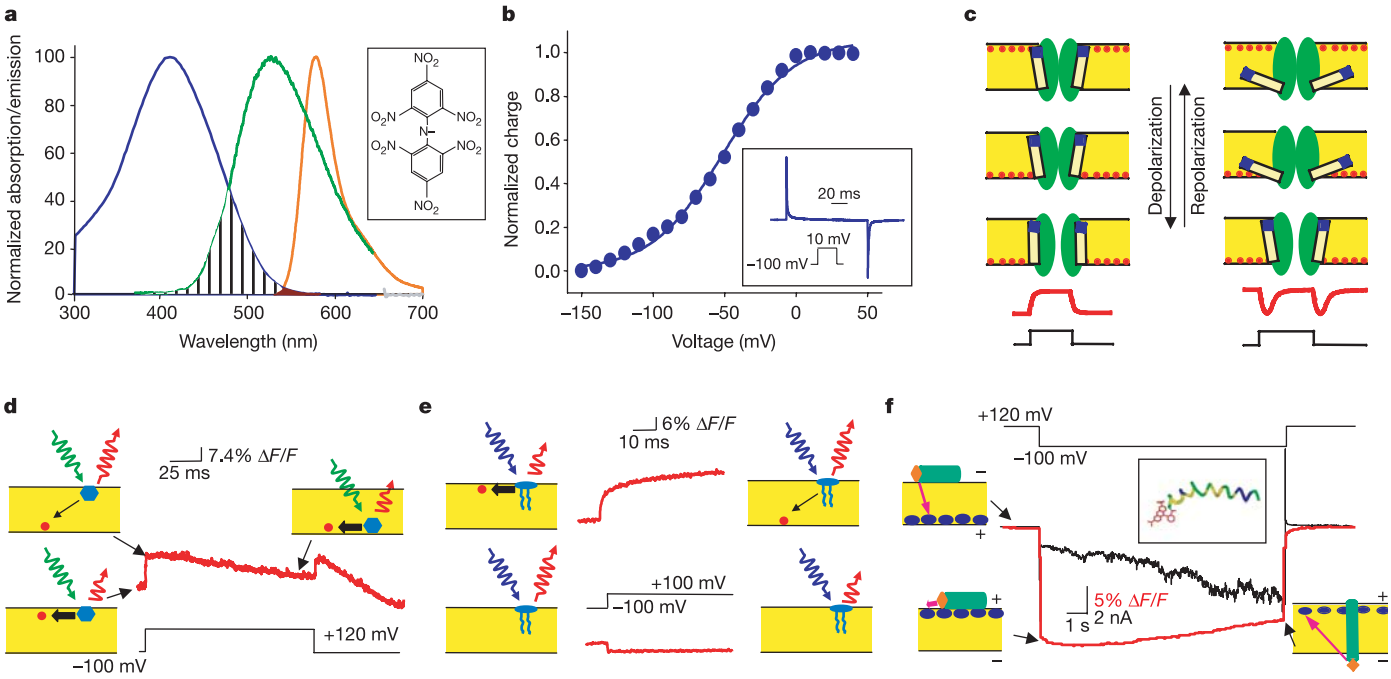

Figure 1 | Voltage-dependent FRET between dipicrylamine and model membrane probes. a, Dipicrylamine (structure shown in inset) absorbance spectra (blue) along with tetramethylrhodamine (orange) and ABD (green) emission spectra. **b**, Charge–voltage relationship of dipicrylamine with a representative gating-current trace (inset). **c**, Schematic representation of molecular movements of dipicrylamine (red circles) and labelled (blue) S4 segments (yellow rectangles) in the channel (green) embedded in the membrane (yellow) based on contrasting models of voltage-gating (left panel, no transmembrane movement; right panel, large transmembrane movement). The time course of the FRET signal (red traces) and the voltage pulses (black traces) in each gating model are shown at the bottom. **d**, The time trace of voltage-dependent FRET (red trace) between the membrane-translocating probe oxonol (blue hexagons) and dipicrylamine (red circles). **e**, Upper panel, the voltage-dependent FRET signal (red trace) between di-8-ANEPPS (blue) and dipicrylamine (red circles). Lower panel, the intrinsic di-8-ANEPPS electrochromic signal (red trace). **f**, The time trace of FRET signal (red trace) between N-TMR-melittin (green cylinder) and dipicrylamine (blue ovals) is overlaid on the current recordings (black trace). Inset, structure of N–TMR–melittin.

rhodamine, is located closer to the outer leaflet, as would be expected from their structural differences. However, like sulphorhodamine, the FRET signal of the ABD–DPA pair is monophasic, confirming that there is no evidence of transmembrane crossing. Our measurements indicate that the residues in the S3b–S4 loop and the S4 segment do not translocate across the bilayer during the gating process.

The lack of significant transmembrane displacement of the S4 segment strongly constrains the type of molecular motions that are able to generate a gating charge of 13*e*. To illustrate the counter-intuitive concept of voltage gating in the context of limited transmembrane movement, we have constructed a molecular model of the Shaker K^+ channel using the X-ray structure of the bacterial channel KvAP (voltage-dependent K^+ channel from *Aeropyrum pernix*) together with the available experimental data (Fig. 3). The channel was modelled conservatively by preserving the overall packing of all α-helical elements of the voltage sensor. The structural details are obviously uncertain owing to the lack of experimental data; however, the most important features of the model are strongly supported by the currently available information. In particular, the R362 residue in S4 is in proximity to the A419 residue in S5 near the extracellular side of the Shaker channel in the activated state[19]. In order to generate 13*e* gating charges upon hyperpolarization in the context of limited inward S4 transmembrane movement, it is necessary for the intracellular electrical potential to extend near the extracellular surface when the channel is in the resting state; presumably through a high dielectric aqueous crevice. This notion—that the transmembrane potential is 'focused' near the extracellular side in the region of the first four gating charges in S4 through an intracellular aqueous cavity—is supported by experimental evidence of a proton-conducting pore in the R362H mutant of the Shaker channel in the closed state[12], the strong dependence of gating charge quantity on intracellular ionic strength[20], and the measurement of an amplified membrane electric field near the second gating charge residue[15].

Figure 3a shows the models of the Shaker K^+ channel in the open and closed state where the out-of-plane subunits have been removed

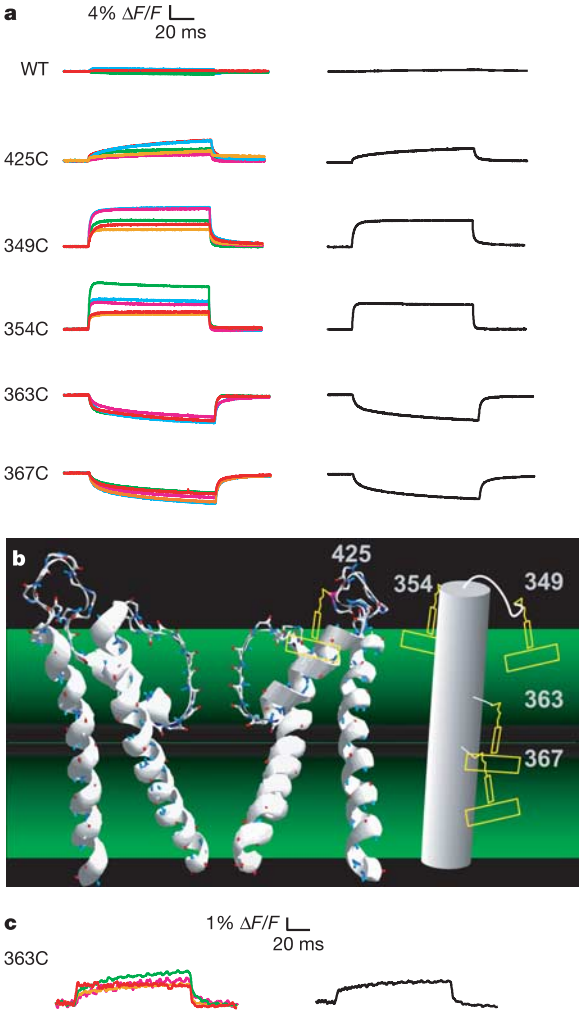

Figure 2 | FRET measurements between labelled Shaker potassium channel and dipicrylamine. a, Time trace of voltage-dependent FRET change of sulphorhodamine measured from different positions in the Shaker channel in response to a voltage pulse to +50 mV from a pre-pulse and a post-pulse of −120 mV. Left, each colour corresponds to a measurement in an individual oocyte; right, average of voltage-dependent FRET from all oocytes. **b**, Cartoon representation of the labelled positions in the Shaker S4 segment and the pore turret. **c**, Time trace of voltage-dependent FRET measured from position V363C labelled with ABD–MTS in response to a pulse to +50 mV from a pre-pulse and post-pulse of − 120 mV. (Left and right panels have the same meaning as in **a**.) WT, wild type.

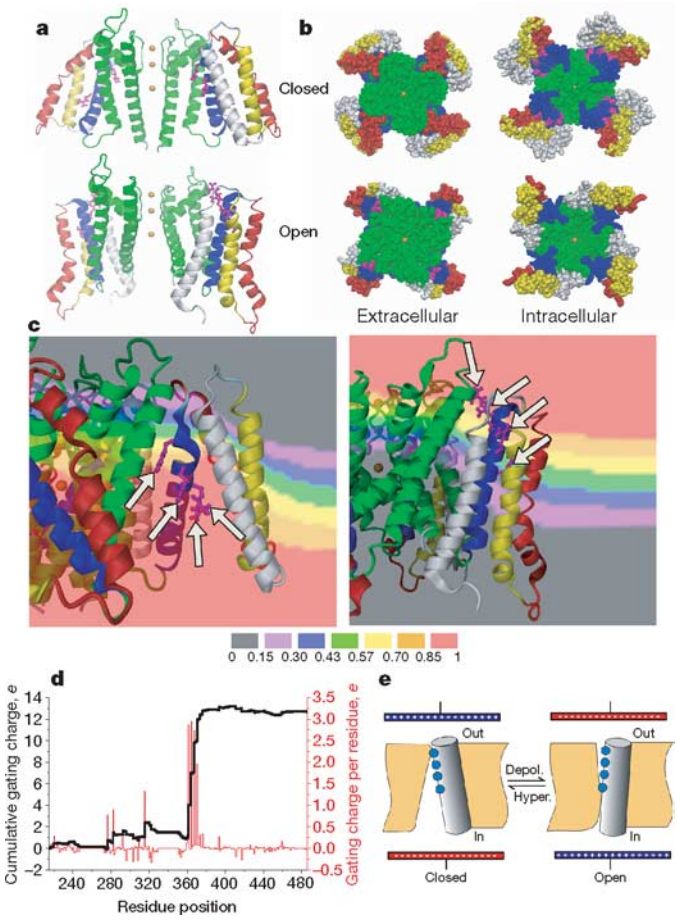

Figure 3 | Molecular model of voltage-gating in Shaker potassium channel. a, Axial view showing two of the four subunits of the Shaker potassium channel embedded in the lipid bilayer in a closed (upper panel) and an open state (lower panel). S1, white; S2, yellow; S3, red; S4, blue; pore region, green; charge-carrying arginine residues, magenta. **b**, Intracellular and extracellular views of the space-filled model of the Shaker potassium channel. **c**, Close-up view of voltage-sensor charges in the closed (left panel) and open state (right panel) overlaid with the isopotential surface. The colour bars (below) correspond to dimensionless fractions of the total transmembrane potential. Arrows highlight the arginine residues. **d**, Gating charge per residue (red) and cumulative gating charge (black) transported across the membrane field as the channel goes from a closed to an open state as a function of residue position. **e**, Schematic of the transporter model of voltage-gating where depolarization alters the accessibility of the charged residues from internal to external water-filled crevices.

for clarity. Figure 3b shows the intra- and extracellular views of the structure, where it is apparent that the arginine residues are visible from the outside in the open state and from the inside in the closed state. The molecular models of the open and closed states of the channel allow for the computation of the gating charge by solving the modified Poisson–Boltzmann equation[21]. A close-up view of the voltage sensor and the iso-potential lines (Fig. 3c) shows that the voltage-sensing arginine residues move across most of the focused electric field by re-orienting the side chains with very little translocation of the voltage-sensor backbone (Fig. 3c). The cumulative charge that is translocated in the Shaker channel, computed as a function of residue position, is shown in Fig. 3d. The structural model is able to quantitatively reproduce the displacement of 12–13 elementary charges contributed by the first four charges on S4, as determined experimentally in the Shaker channel[1,2], without the requirement for large transmembrane movements of S4. In this model, the S4 backbone undergoes a 45° change in tilt upon gating but translates only a short distance (less than 2 Å) perpendicular to the membrane, while the charges are relocated from a deep internally facing aqueous crevice in the closed state to an external crevice when it opens (Fig. 3). In the open state, the intracellular crevice that is apparent in the closed state essentially disappears, as the S1–S4 segments pack into a tight helical bundle. The residues near the S3–S4 loop (I325–R371) that form the structural helix–turn–helix paddle motif in the X-ray structure of KvAP move together as a stable dynamic unit (a difference of only 3 Å root mean square deviation, r.m.s.d., for the Cα between the modelled open and closed state), with the carboxy terminus of S3 serving to electrically insulate S4 from the extracellular side in the closed state.

These results suggest that the operation of the voltage sensor could be qualitatively similar to a transporter, in which the accessibility to a binding site alternates between the inside and outside with each transport cycle[22]. In the case of voltage-gated ion channels, the charged arginine residues are analogous to 'tethered substrates' whose accessibility alternates as a function of membrane voltage (Fig. 3e). Thus, an evolutionarily conserved transporter-like mechanism may be sufficient to move the large amount of charge across the electric field that is required for the steep voltage dependence of voltage-gated channels, without translocating the S4 segment across the membrane.

Note added in proof: The atomic structure of Kv1.2 determined by X-ray crystallography appeared online while this publication was in press[31]. Despite some differences, the current model of Shaker in the open state is broadly consistent with the structure of Kv1.2, and the calculated gating charge is not expected to change (see Supplementary Discussion).

METHODS

Molecular biology and labelling. All the Shaker-channel constructs used in this work were generated in an inactivation-removed (Δ6–46 ShH4) non-conducting (W434F) cysteine-less (C96S/C245V/C286V/C301S/C308S/C462A/C505S) channel background[23]. Site-directed mutagenesis, *in vitro* transcription, complementary RNA injections and labellings were performed as described previously[24] with small modifications. Labelling with methanethiosulphonate–(MTS)–sulphorhodamine (Toronto Research Chemicals) and 7-fluorobenz-2-oxa-1,3-diazole-4-sulphonamide (ABD)–MTS (Toronto Research Chemicals) was performed for 5 min on ice, whereas *N*-(3-sulphopropyl)-4-(2-(6-*N*,*N*-dioctyl-beta-aminonaphthalene)ethenyl)pyridinium (di-8-ANEPPS; Molecular Probes) was at room temperature (20–22 °C). During recording, the external solution was perfused with 20 μM of DPA. FRET measurements of oxonol–DPA were in presence of 2 μM bis-(1,3-diethylthiobarbituric acid)trimethine oxonol (Molecular Probes).

FRET measurements in cut-open oocytes. Time-resolved FRET measurements under voltage-clamp conditions between labelled Shaker channels and DPA were carried out in a modified cut-open oocyte set-up using customized acquisition and analysis systems described previously[25]. Sulphorhodamine and oxonol fluorescence was measured using standard tetramethylrhodamine (TMR) optics[24], whereas di-8-ANEPPS fluorescence measurements used a 425 nm/50 nm band pass (BP) excitation filter. ABD fluorescence was excited with a filter cube consisting of a 425 nm/50 nm BP excitation filter, a 475 nm long pass dichroic filter with no emission filters. Voltage-dependent FRET signals from the expressed channels were generated by subtracting the average FRET signal obtained in uninjected oocytes within the same batch. All FRET changes ($\Delta F/F$) were normalized to the background fluorescence before adding DPA. The R_o in FRET measurements is defined as the distance corresponding to 50% efficiency for a specific donor–acceptor pair. The calculated R_o for the sulphorhodamine–dipicrylamine pair was 22 Å and the ABD–dipicrylamine pair was 23 Å. The Q_D (the quantum yield of the donor) of ABD in ethanol was 0.18.

FRET measurements in planar lipid bilayers. Bilayer fluorescence was recorded using a horizontal bilayer set-up mounted on an inverted microscope. Fluorophores were excited with de-focused laser light ($\lambda = 514$ nm) and fluorescence (emission filter 610 nm/75 nm BP) recorded with a Cascade charge-coupled device (CCD) camera (Roper Scientific). Bilayers were formed from a 3:1mixture of 1-palmitoyl-2-oleoyl-*sn*-glycero-3-phosphocholine:1-palmitoyl-2-oleoyl-*sn*-glycero-3-phosphoethanolamine (POPC:POPE; Avanti Polar Lipids) in decane (25 mg ml^{-1}). Melittin labelled at the N-terminus with tetramethylrhodamine (N–TMR–melittin; Alpha Diagnostics International) was added to the top (outside) chamber (concentration, 10 μM). Voltage convention is inside potential minus outside potential.

Molecular modelling and Poisson–Boltzmann calculations. The Shaker model was constructed as described previously[19]. Briefly, the structure of the S1 through S4 crystal was docked to the pore region of the full crystal structure of KvAP (ref. 8) for the open state, and to the KcsA (ref. 26) for the S5–S6 pore structure of the closed state. To avoid ambiguous insertions in the homology modelling, the Shaker S3–S4 loop was shortened to eight residues[27]. The r.m.s.d. relative to the X-ray structure of the isolated voltage sensor of KvAP is 6 Å and 9 Å (Cα) for the open and closed states, respectively. Models were refined by energy minimization and molecular dynamics simulations using the program CHARMM (ref. 28). Gating charge was calculated from the structural models using the modified Poisson–Boltzmann voltage equation[21] implemented in the finite-difference PBEQ module of CHARMM. A dielectric of 2 was assigned to the protein, and the protein–solvent interface was determined using the set of optimized atomic Born radii[29]. The membrane was represented as a 24 Å slab of low dielectric 2, assembled by packing neutral spheres around the channel; all aqueous crevices of the pore and voltage sensor were represented as high dielectric regions of 80. A 1 Å grid was used. S4 is significantly exposed to the membrane (~20%), although the arginine residues are exposed to aqueous regions in agreement with electron paramagnetic resonance results in KvAP (ref. 30). The volume of the intracellular crevice of the closed state, which is partly bounded by the membrane, corresponds to 30–40 water molecules, in accord with experimental estimates[20]. Figure 3c was created using the DINO3D software (www.dino3d.org).

Received 6 April; accepted 6 June 2005.

1. Aggarwal, S. K. & MacKinnon, R. Contribution of the S4 segment to gating charge in the Shaker K^+ channel. *Neuron* **16,** 1169–1177 (1996).
2. Seoh, S. A., Sigg, D., Papazian, D. M. & Bezanilla, F. Voltage-sensing residues in the S2 and S4 segments of the Shaker K^+ channel. *Neuron* **16,** 1159–1167 (1996).
3. Bezanilla, F. The voltage sensor in voltage-dependent ion channels. *Physiol. Rev.* **80,** 555–592 (2000).
4. Ahern, C. A. & Horn, R. Stirring up controversy with a voltage sensor paddle. *Trends Neurosci.* **27,** 303–307 (2004).
5. Jiang, Y., Ruta, V., Chen, J., Lee, A. & MacKinnon, R. The principle of gating charge movement in a voltage-dependent K(+) channel. *Nature* **423,** 42–48 (2003).
6. Guy, H. R. & Seetharamulu, P. Molecular model of the action potential sodium channel. *Proc. Natl Acad. Sci. USA* **83,** 508–512 (1986).
7. Catterall, W. A. Molecular properties of voltage-sensitive sodium channels. *Annu. Rev. Biochem.* **55,** 953–985 (1986).
8. Jiang, Y. *et al.* X-ray structure of a voltage-dependent K(+) channel. *Nature* **423,** 33–41 (2003).
9. Yang, N., George, A. L. Jr & Horn, R. Molecular basis of charge movement in voltage-gated sodium channels. *Neuron* **16,** 113–122 (1996).
10. Larsson, H. P., Baker, O. S., Dhillon, D. S. & Isacoff, E. Y. Transmembrane movement of the shaker K^+ channel S4. *Neuron* **16,** 387–397 (1996).
11. Starace, D. M., Stefani, E. & Bezanilla, F. Voltage-dependent proton transport by the voltage sensor of the Shaker K^+ channel. *Neuron* **19,** 1319–1327 (1997).
12. Starace, D. M. & Bezanilla, F. A proton pore in a potassium channel voltage sensor reveals a focused electric field. *Nature* **427,** 548–553 (2004).
13. Cha, A., Snyder, G. E., Selvin, P. R. & Bezanilla, F. Atomic scale movement of the voltage-sensing region in a potassium channel measured via spectroscopy. *Nature* **402,** 809–813 (1999).
14. Glauner, K. S., Mannuzzu, L. M., Gandhi, C. S. & Isacoff, E. Y. Spectroscopic

mapping of voltage sensor movement in the Shaker potassium channel. *Nature* **402,** 813–817 (1999).
15. Asamoah, O. K., Wuskell, J. P., Loew, L. M. & Bezanilla, F. A fluorometric approach to local electric field measurements in a voltage-gated ion channel. *Neuron* **37,** 85–97 (2003).
16. Gonzalez, J. E. & Tsien, R. Y. Voltage sensing by fluorescence resonance energy transfer in single cells. *Biophys. J.* **69,** 1272–1280 (1995).
17. Tosteson, M. T. & Tosteson, D. C. The sting. Melittin forms channels in lipid bilayers. *Biophys. J.* **36,** 109–116 (1981).
18. Kempf, C. *et al.* Voltage-dependent trans-bilayer orientation of melittin. *J. Biol. Chem.* **257,** 2469–2476 (1982).
19. Laine, M. *et al.* Atomic proximity between S4 segment and pore domain in Shaker potassium channels. *Neuron* **39,** 467–481 (2003).
20. Islas, L. D. & Sigworth, F. J. Electrostatics and the gating pore of Shaker potassium channels. *J. Gen. Physiol.* **117,** 69–89 (2001).
21. Roux, B. Influence of the membrane potential on the free energy of an intrinsic protein. *Biophys. J.* **73,** 2980–2989 (1997).
22. Abramson, J. *et al.* Structure and mechanism of the lactose permease of *Escherichia coli*. *Science* **301,** 610–615 (2003).
23. Boland, L. M., Jurman, M. E. & Yellen, G. Cysteines in the Shaker K^+ channel are not essential for channel activity or zinc modulation. *Biophys. J.* **66,** 694–699 (1994).
24. Chanda, B. & Bezanilla, F. Tracking voltage-dependent conformational changes in skeletal muscle sodium channel during activation. *J. Gen. Physiol.* **120,** 629–645 (2002).
25. Cha, A. & Bezanilla, F. Structural implications of fluorescence quenching in the Shaker K^+ channel. *J. Gen. Physiol.* **112,** 391–408 (1998).
26. Zhou, Y., Morais-Cabral, J. H., Kaufman, A. & MacKinnon, R. Chemistry of ion coordination and hydration revealed by a K^+ channel-Fab complex at 2.0Å resolution. *Nature* **414,** 43–48 (2001).
27. Gonzalez, C., Rosenman, E., Bezanilla, F., Alvarez, O. & Latorre, R. Periodic perturbations in Shaker K^+ channel gating kinetics by deletions in the S3–S4 linker. *Proc. Natl Acad. Sci. USA* **98,** 9617–9623 (2001).
28. Brooks, B. R. *et al.* CHARMM: A program for macromolecular energy, minimization, and dynamics calculations. *J. Comput. Chem.* **4,** 187–217 (1983).
29. Nina, M., Beglov, D. & Roux, B. Atomic Born radii for continuum electrostatic calculations based on molecular dynamics free energy simulations. *J. Phys. Chem. B* **101,** 5239–5248 (1997).
30. Cuello, L. G., Cortes, D. M. & Perozo, E. Molecular architecture of the KvAP voltage-dependent K^+ channel in a lipid bilayer. *Science* **306,** 491–495 (2004).
31. Long, S. B., Campbell, E. B. & MacKinnon, R. Crystal structure of a mammalian voltage-dependent *Shaker* family K^+ channel. *Science* 7 July 2005 (doi:10.1126/science.1116269).

Supplementary Information is linked to the online version of the paper at www.nature.com/nature.

Acknowledgements We thank M. J. Hahn for technical assistance, M. Holmgren for the cysteine-less Shaker clone, W. Hubell for the gift of dipicrylamine and the members of Bezanilla and Correa laboratories for their comments. This work was supported by funds from an AHA postdoctoral fellowship to B.C., NRSA funding to O.K.A, DFG funding to R.B. and an NIH grant to F.B.

Author Information Reprints and permissions information is available at npg.nature.com/reprintsandpermissions. The authors declare no competing financial interests. Correspondence and requests for materials should be addressed to F.B. (fbezanil@ucla.edu)